J Nanopart Res (2011) 13:931–937
DOI 10.1007/s11051-010-0197-7

BRIEF COMMUNICATION

Pumping power of nanofluids in a flowing system

Jules L. Routbort · Dileep Singh · Elena V. Timofeeva · Wenhua Yu · David M. France

Received: 24 August 2010 / Accepted: 20 December 2010 / Published online: 14 January 2011

Abstract Nanofluids have the potential to increase thermal conductivities and heat transfer coefficients compared to their base fluids. However, the addition of nanoparticles to a fluid also increases the viscosity and therefore increases the power required to pump the fluid through the system. When the benefit of the increased heat transfer is larger than the penalty of the increased pumping power, the nanofluid has the potential for commercial viability. The pumping power for nanofluids has been considered previously for flow in straight tubes. In this study, the pumping power was measured for nanofluids flowing in a complete system including straight tubing, elbows, and expansions. The objective was to determine the significance of two-phase flow effects on system performance. Two types of nanofluids were used in this study: a water-based nanofluid containing 2.0–8.0 vol% of 40-nm alumina nanoparticles, and a 50/50 ethylene glycol/water mixture-based nanofluid containing 2.2 vol% of 29-nm SiC nanoparticles. All experiments were performed in the turbulent flow region in the entire test system simulating features typically found in heat exchanger systems. Experimental results were compared to the pumping power calculated from a mathematical model of the system to evaluate the system effects. The pumping power results were also combined with the heat transfer enhancement to evaluate the viability of the two nanofluids.

Keywords Nanofluids · Fluid flow · Pumping power · Nanoparticle · Colloids

J. L. Routbort (✉) · E. V. Timofeeva · W. Yu
Energy Systems Division, Argonne National Laboratory, Argonne, IL 60439, USA
e-mail: routbort@anl.gov

D. Singh
Nuclear Engineering Division, Argonne National Laboratory, Argonne, IL 60439, USA

D. M. France
Deptment of Mechanical and Industrial Engineering, University of Illinois at Chicago, Chicago, IL 60607, USA

Introduction

Most fluids containing solid nanoparticles have been shown to possess enhanced thermal conductivities compared to their base fluids, and therefore there exists the possibility to have increased heat transfer coefficients (Yu et al. 2008). On the other hand, the addition of nanoparticles to a fluid also increases its viscosity (Vold and Vold 1983). The increased viscosity will result in an increase in the power required to pump the nanofluid at the same velocity as the base fluid as has been reported for 5 vol% of Al_2O_3, CuO, and diamond nanoparticles in water (Torii 2010). However, if the heat transfer of a nanofluid is much higher than that of the base fluid, the nanofluid could be pumped at a lower velocity than that of the base fluid while maintaining the same

heat transfer rate. The magnitudes of both the heat transfer coefficient and the pumping power for a particular application are required to determine the viability of a nanofluid. The objective of this study was to measure and to evaluate pumping power requirements for nanofluids in a closed flow system.

Nanofluids consisting of nanometer-sized alumina particles suspended in water have been used in many experiments to study general characteristics of nanofluids, and many results are available in the literature. Heat transfer and pressure-drop studies showed that alumina/water nanofluids usually have moderate enhancements of the thermal conductivity and are not optimum for heat transfer applications (Yu et al. 2008). The ratio of heat transfer coefficient of an alumina/water nanofluid to the base fluid usually is <1 mainly due to the significant viscosity increase in the alumina suspension (Yu et al. 2008, 2010). However, previous investigations have reported general nanofluid results using alumina-based nanofluids, and they were one type used in this study for which extensive viscosity and thermal conductivity measurements have been made (Timofeeva et al. 2009). The alumina particles used in this study have a fairly uniform size, stay in suspension well, and make a good nanofluid for comparing experimental results to calculations.

There have been several nanofluid studies in which the pressure drop, from which the pumping power can be calculated, was measured in straight tubes. Torii (2010) measured pressure drop using 5 vol% concentrations of three nanofluids including alumina in water under turbulent flow conditions. Measured pressure-drop values were "reasonably predicted" using a standard liquid friction factor model with nanofluid properties. Xuan and Li (2003) reported pressure-drop measurements for turbulent flow of nanofluids in a straight tube in terms of the friction factor. The results showed that the friction factor was a function of the nanofluid Reynolds number, and it was concluded that it could be predicted from the friction factor correlation for the single-phase flow. These results imply that, for pressure-drop considerations in a straight tube, the two-phase nanofluid flow acts like a liquid. That was also the general conclusion of Williams et al. (2008) where two nanofluids, including alumina in water, were tested in turbulent flow in a straight tube, and predictions of the pressure drop were within 20% of measurements.

The pressure-drop results discussed above were all for flow in straight tubes. However, flow systems include components like elbows and transitions in which the particle momentum can have an increased influence on the pressure drop. It is not known to what degree nanoparticles follow streamlines in such components. Flow around a 90° elbow, for example, can result in higher particle concentrations near the outside radius and particle interactions with the wall. The magnitude of such effects on the pressure drop has not been determined for nanofluids. Therefore, in this study, the pumping power was measured in a test system with components typical of closed flow systems associated with heat exchangers. The objective was to determine if the pumping power of a nanofluid flowing in a closed system could be predicted from liquid equations using properties of the nanofluid as is the case for flowing in straight tubes. These experiments were designed to determine whether two-phase flow phenomena are significant for the pumping power determination of complete fluid systems or liquid predictions similar to the straight tube case are reasonable. To that end, the torque, and thus the pumping power, required to pump alumina/water nanofluids at particle concentrations from 2 to 8 vol% was measured. For comparison, measurements were also made of the torque required to pump a higher viscosity nanofluid: 2.2 vol%, 29-nm α-SiC in a 50/50 ethylene glycol/water mixture (Timofeeva et al. 2011).

Experimental

Materials

The boehmite (α-AlOOH) alumina used in this investigation has been well described and characterized (Timofeeva et al. 2009). The material (tradename Catapal-200) was donated by Sasol North America Inc., and was in the shape of bricks or cubes with a dimension of 40 nm. Small-angle X-ray scattering, dynamic laser scattering, and XRD measurements were in good agreement with the manufacturer's specification of $\sim$40 nm (Timofeeva et al. 2009).

Table 1 Basic properties of the nanofluids at 25 °C

Vol%	Viscosity (cP)	Density (kg/m^3)	Thermal conductivity (W/mK)	Specific heat (J/kg K)	Mo ratio (25 °C)
Water	0.89	997	0.587	4186.0	1
2.0 alumina	1.12	1038	0.618	4078.0	0.945
4.0 alumina	1.29	1082	0.654	3974.5	0.929
8.0 alumina	2.10	1158	0.712	3293.8	0.86
EG/H_2O	3.35	1056	0.381	3300.0	1
2.2 SiC	4.10	1098	0.437	3036.4	0.98

The heat transfer efficiency is calculated as ratios of Mo-nanofluid/Mo-base fluid. The specific heat was calculated from the rule of mixtures

Alumina particles were dispersed in distilled water with particle concentrations of 2, 4, and 8 vol% and the pH was adjusted to 3.2 ± 0.5. The viscosity of the alumina nanofluids was measured to ±5% using a Brookfield DV-II+ rotational-type viscometer with the SC4–18 spindle. The thermal conductivity was measured by a KD2Pro thermal property analyzer (Decagon Devices Inc.). The density was measured by weighting the aliquot of the suspension. The results of the nanofluid property measurements are given in Table 1.

The nanofluid of a 2.2 vol% SiC in a 50/50 ethylene glycol/water mixture was prepared from a water-based suspension of α-SiC particles (Saint Gobain Inc.) with average sizes determined from BET of 29 nm (Timofeeva et al. 2010). The pH was maintained at 9.5 ± 0.3 to engage the electrostatic stabilization of the suspension and to minimize the viscosity increase.

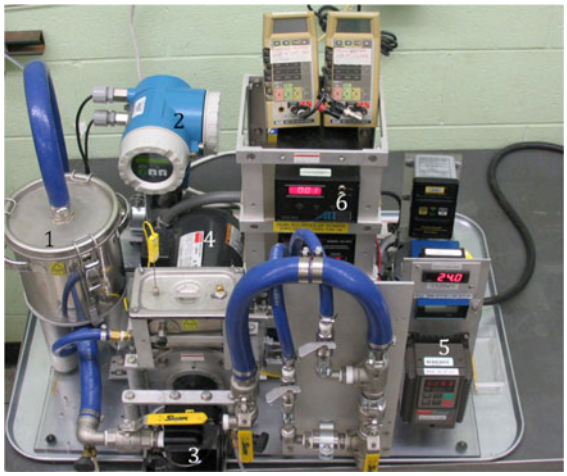

Fig. 1 The photograph of the erosion/torque apparatus with principal parts used for torque measurement. *1* nanofluid reservoir and piping system, *2* magnetic flow meter, *3* automotive water pump with removable impellor, *4* pump motor, *5* motor controller and rpm readout, and *6* torque readout

Methods

An apparatus, originally designed to measure the erosion of materials by nanofluids, was modified by inclusion of a torque meter with a wireless pickup. A photograph of the apparatus is shown in Fig. 1. The principal components of the system are: (1) nanofluid reservoir and piping system, (2) magnetic flow meter (Promag 53, manufactured by Endress+Hauser, Greenwood, IN), (3) automotive water pump with removable impellor, (4) pump motor, (5) motor controller and rpm readout, and (6) torque readout. A calibrated torque meter with wireless pickup (ATI, Spring Valley, Ohio) and data logger are hidden behind the frame and the steel tank (only used for erosion measurements). The data logger records the torque 500 times/s and sends the measurements to Labview on a PC. All measurements were made at ambient temperatures of 30 ± 2 °C that is measured in the reservoir and recorded on the meter mounted near the motor controller. A typical torque measurement is shown in Fig. 2. The results to be shown later are the average of 2–4 measurements accumulated over a period of ≈30 min (as shown in Fig. 2) and taken in both ascending and descending order of flow rates that were between 21 and 28 L/min. The apparatus was thoroughly cleaned after experiments with each nanofluid were completed, and water data were reproduced before starting measurements on the next nanofluid.

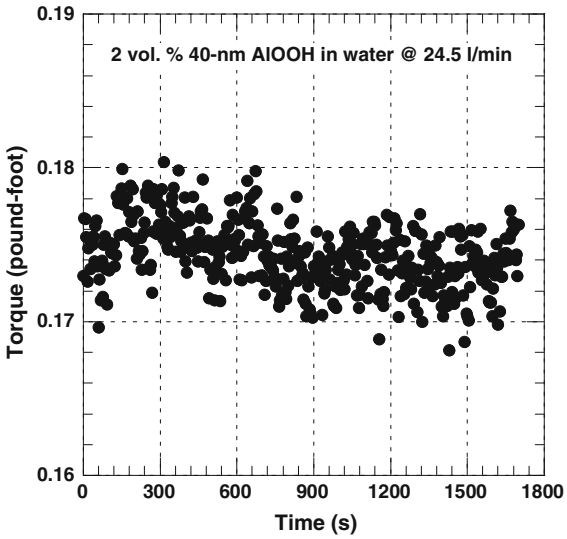

Fig. 2 The torque is shown as a function of time for the 2.0 vol% alumina/water nanofluid at a flow rate of 24.5 L/min. Each point represents the average of 500 readings. The rpm of the pump was 1700

Calculation of power

The shaft power P_{shaft} is the product of the torque τ and the angular velocity ω and can be expressed as a function of the pumping power P_{pumping} through the pump efficiency η

$$P_{\text{shaft}} = \tau\omega = P_{\text{pumping}}/\eta. \tag{1}$$

In the above equation, the pumping power for a fluid with density ρ and viscosity μ can be expressed as the product of the volumetric flow rate Q and the pressure drop Δp

$$P_{\text{pumping}} = Q\Delta p, \tag{2}$$

where the volumetric flow rate can be expressed as a function of velocity V through the cross section area A or the circular tube diameter d

$$Q = AV = \left(\pi d^2/4\right)V. \tag{3}$$

For a continuously flowing system, the pressure drop usually includes the static head as a function of vertical position h ($\Delta p_{\text{static}} = \rho gh$), the friction pressure drop as a function of the friction factor f and the tube length L ($\Delta p_{\text{friction}} = 2\rho V^2(L/d)f$), and other pressure losses due to elbows, expansions, contractions, and a variety of other components. By expressing the component pressure losses in terms of the component inlet velocity V_i, the shaft power for a turbulent fluid flow can be expressed as (Fox et al. 2008)

$$P_{shaft} = \frac{Q\Delta p}{\eta} = \frac{\left(\pi d^2/4\right)V\left[\rho gh + 2\rho V^2(L/d)f + \sum_i K_i(1/2)\rho V_i^2\right]}{\eta}, \tag{4}$$

where the pressure loss coefficient K_i is determined by the nature of a pressure loss component (Fox et al. 2008) and the Fanning friction factor f depends on the flow conditions and can be estimated through the Reynolds number Re by the Blasius equation for a turbulent fluid flow as (Blasius 1913).

$$f = 0.791\ \text{Re}^{-0.25} = 0.0791(\rho Vd/\mu)^{-0.25}. \tag{5}$$

The data from this study will be presented in terms of measured torque and the torque ratio of the nanofluid to the base fluid for both the measured data and the calculated values. The ratio of the calculated torque of the nanofluid to the calculated torque of the base fluid, $\tau_{\text{nf}}/\tau_{\text{bf}}$, at a constant velocity, V, was determined using Eq. 4 with a somewhat simplified system model, all in the turbulent flow region. The comparisons assumed that the pump efficiencies for the nanofluid and base fluid are equal.

Results and discussion

The experimental flow system shown in Fig. 1 consists of small radius 90° elbows, pipes and tubing, expansions and contractions, and a variety of other components discussed previously. A simplified flow model was developed for the system consisting of a straight smooth pipe (2 m in length), five small radius 90° elbows, and two abrupt expansions. These eight components were used as the model for calculating the pressure drop through the system per Eq. 4. In all cases, the ratio was taken of the pumping power of the nanofluid, calculated from the product of the pressure drop and the volumetric flow rate, to the pumping power of the base fluid. That ratio was rather insensitive to the simplicity of the flow model of the experimental system. For example, doubling the pipe length in the model (a marked deviation from

reality) produced almost no measurable change in the pumping power ratio prediction. Therefore, the simplified model adequately describes the actual pumping system.

The purpose of the system model, from which the pumping power was calculated from the fluid parameters, was to serve as a comparison with the torque measurement determination of the pumping power. The differences between the two pumping powers could be attributed to the characteristics of the nanofluids beyond what can be predicted for a pure liquid with properties of the suspensions. Such differences, which may occur due to the fluid mechanics of two-phase flow through system components such as 90° elbows and expansions, have not been considered before this study. Such differences occur with respect to the nanofluid viscosity and have occasionally been reported to lesser extents for the thermal conductivity and the heat transfer coefficient (Yu et al. 2008).

Figure 3 presents the experimentally measured values of the torque versus the flow rate for the 2, 4, and 8 vol% water-based alumina nanofluids. All measurements were made in the turbulent region with the Reynolds numbers between 14,600 and 24,600. The data for the base fluid, water, are reproducible to about ±2%, while the nanofluids seem to have more scattered possibly as a result of particle separation due to the centripetal force caused by the pump impellor. The viscosity of the most concentrated nanofluid (8 vol% alumina), where agglomeration is most probable, showed Newtonian behavior with no shear thinning. It should be mentioned that we are operating at the lower range of the torque meter, and the shaft of the pump is not completely concentric to the axis of the torque meter. Those factors could account for some of the scatter. Over the limited range of flow rates measured between 21 and 28 L/min, and within the ±5% experimental uncertainty, the ratio of the torque required to pump the nanofluids to that of the base fluid is nearly independent of the flow rate.

Figure 4 presents the results of the ratio of the measured torque of the nanofluids to the measured torque of the base fluid (water), τ_{nf}/τ_{bf}, at a constant velocity V with a flow rate of 25 L/min. That ratio is compared to the calculated ratio using Eq. 4. The error bars reflect the ±5% uncertainty in the torque measurements of the nanofluids and the ±2% uncertainty in the base fluid. The experimental torque increases ~25% in the 2 vol% alumina suspension and only ~35% in the 8 vol% alumina suspension. Unlike the calculated values, these measured torque increases are not linearly proportional to the particle

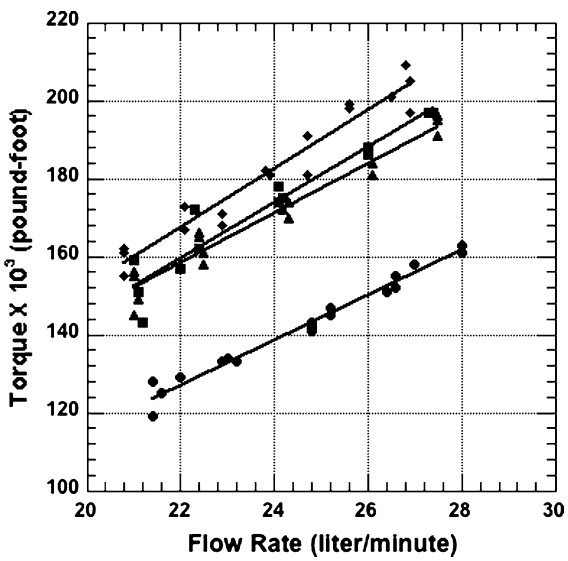

Fig. 3 The measured torque versus the flow rate for water (*circles*), 2 vol% alumina in water (*triangles*), 4 vol% alumina in water (*squares*), and 8 vol% alumina in water (*diamonds*)

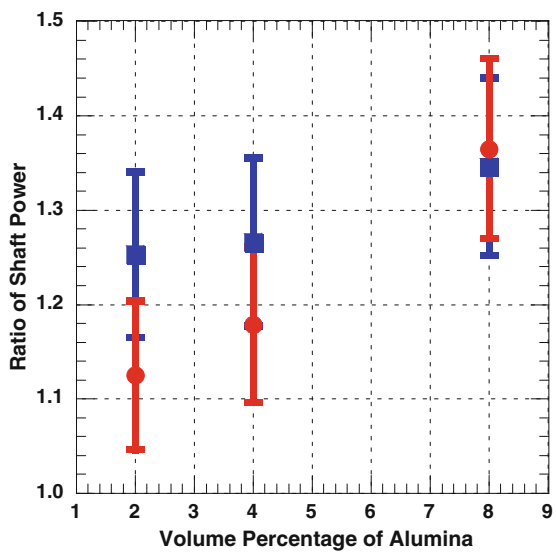

Fig. 4 The ratio of the shaft power for the alumina nanofluids to the base fluid for measured (*squares*) and calculated (*circles*) with the flow rate of 25 L/min

concentration. Considering all contributing uncertainties in the measured torque values, it is noteworthy that the calculated values and the experimental data overlap. The discrepancy is larger for lower concentrations of alumina than for the higher concentrations of alumina. For the 8 vol% alumina suspension, there is a good agreement between the calculated values and the experimental measurements. Because calculated pumping power values are very sensitive to the viscosity per Eq. 4, the discrepancy for the 2 and 4 vol% water-based alumina nanofluids in part is the result of the higher uncertainties of measuring their lower viscosities.

As a check on the viscosity measurement uncertainty, we measured the torque required to pump the 2.2 vol% 29-nm SiC (Timofeeva et al. 2010) in 50/50 ethylene glycol/water mixture (Fig. 5). The viscosity of this fluid is about four times higher than that of the 2 and 4 vol% water-based alumina nanofluids. The increase in torque compared to that of the base fluid, 50/50 ethylene glycol/water, was independent of the flow rate in the range of 20–26 L/min, and the percentage increase in torque was 9.3% while the calculated percentage increase was 8.7%. This agreement is consistent with the agreement found for the higher viscosity 8 vol% water-based alumina nanofluid reported above. These comparisons support the procedure of making pumping power calculations for

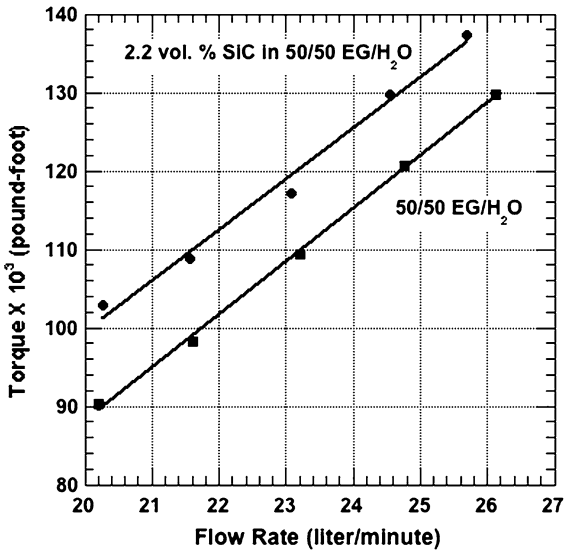

Fig. 5 The torque versus the flow rate for the 2.2 vol% 29-nm SiC in 50/50 ethylene glycol/water compared to the base fluid, 50/50 ethylene glycol/water

nanofluids flowing in closed systems in the same way as for straight tubes, i.e., using liquid equations with the properties of the two-phase nanofluid suspensions.

As discussed previously, the viability of a nanofluid for a specific application depends on both the pumping power and the heat transfer rate. The heat transfer efficiency of a fluid can be estimated from basic properties: thermal conductivity k, viscosity μ, specific heat C_p, and density ρ (Yu et al. 2010). The efficiencies of the alumina/water nanofluids and the SiC–ethylene glycol/water nanofluid were estimated from the Mouromtseff number, Mo. The Mouromtseff number, defined as $\mathrm{Mo} = \rho^{0.8} C_p^{0.4} k^{0.6} \Big/ \mu^{0.4}$, is a figure of merit representing the effectiveness of the nanofluid for turbulent flow (Mouromtseff 1942). Table 1 lists the ratios of Mo-nanofluid/Mo-base fluid for the nanofluids of this study. One can see that, despite the promising increase in the thermal conductivity, the heat transfer efficiency of the alumina/water nanofluids tested in this study are 5 to $\sim$14% worse than that of pure water at room temperature. Considering the $\sim$25–35% increase in the pumping power, it is noteworthy that under conditions of this study, alumina nanofluids are not attractive as commercial heat transfer fluids.

On the other hand, it has been reported that the viscosity of nanofluids decreases with increasing temperature, and the heat transfer efficiency increases (Timofeeva et al. 2011). The nanofluid heat transfer efficiency of the SiC in 50/50 ethylene glycol/water mixture tested in this study is only 2% less than that of the base fluid at room temperature and turns out to be 3% better than that of pure 50/50 ethylene glycol/water mixture at 75 °C. The pumping power will also decrease with rising temperatures as a result of the viscosity decrease, so the SiC–50/50 ethylene glycol/water nanofluid has the potential of overcoming the pumping power penalty with the increased heat transfer efficiency at higher temperatures. The use of larger particles at the same volume concentration also reduces the nanofluid viscosity and improves the heat transfer efficiency (Timofeeva et al. 2010, 2011). Thus, increasing the size of SiC nanoparticles along with higher temperature operation has the potential to overcome the pumping power penalty associated with SiC nanofluids, which can ultimately result in viable heat transfer fluids.

Conclusions

Comparisons of the measured and calculated pumping power ratios of the nanofluids to the base fluids showed that the nanofluids of this study can be considered as single-phase liquids with nanofluid properties for the purpose of pumping power calculations in flow systems consisting of piping, elbows, and expansions. Within limits, the ratios were found to be rather insensitive to the fluid flow rate and the system model. However, the measurements and calculations showed the best agreement for higher viscosity nanofluids where the viscosity measurements were most accurate. The pumping power ratios for the highest viscosity water-based alumina nanofluid (8 vol%) and the ethylene glycol/water-based SiC nanofluid were both very well predicted. Hence for the purpose of pumping power calculations, higher viscosity nanofluids can be treated simply as pure liquids with the properties of the suspensions, and this condition may be extended to lower viscosity nanofluids as far as the viscosity of the nanofluids can accurately be determined. It was also found that the magnitude of the pumping power penalty and the heat transfer enhancement for SiC nanofluids shows potential for producing viable heat transfer fluids.

Acknowledgments The authors are grateful to Drs. Steve Hartline of Saint-Gobain and Yun Chang of Sasol North America Inc., for supplying the SiC–water nanofluid and the alumina nanoparticles, respectively. Roger Smith was instrumental in the design and construction of the apparatus. This work was sponsored by the Office of Vehicle Technologies and the Industrial Technology Program of the US Department of Energy under contract number DE-AC02-06CH11357.

References

Blasius H (1913) Das Ähnlichkeitsgesetz bei Reibungsvorgängen in Flüssigkeiten, Forschungsarbeiten des Ingenieurwesens. Heft 131. Verein Deutscher Ingenieure, Berlin

Fox R, McDonald A, Pritchard P (2008) Introduction to fluid mechanics, 7th edn. Wiley, New Jersey

Mouromtseff IE (1942) Water and forced-air cooling of vacuum tubes. Proc Inst Radio Eng 30:190–205

Timofeeva EV, Routbort JL, Singh D (2009) Particle shape effects on thermophysical properties of alumina nanofluid. J Appl Phys 106:014304

Timofeeva EV, Smith DS, Yu W, France DM, Singh D, Routbort JL (2010) Particle size and interfacial effects on thermo-physical and heat transfer characteristics of water-based α-SiC nanofluids. Nanotechnology 21:215703

Timofeeva E, Yu W, France DM, Singh D, Routbort JL (2011) Base fluid and temperature effects on the heat-transfer characteristics of SiC nanofluids in EG/H_2O and H_2O. J Applied Physics 109 (in press)

Torii S (2010) Turbulent heat transfer behavior of nanofluid in a circular tube heated under constant heat flux. Adv Mech Eng 2010:917612

Vold RD, Vold MJ (1983) Colloid and interface chemistry. Addison-Wesley, Reading

Williams W, Buongiorno J, Hu L-W (2008) Experimental investigation of turbulent convective heat transfer and pressure loss of alumina/water and zironia/water nanoparticle colloids (nanofluids) in horizontal tubes. J Heat Transfer 130:042412

Xuan Y, Li Q (2003) Investigation on convective heat transfer and flow features of nanfluids. J Heat Transf 125:151–155

Yu W, France DM, Routbort JL, Choi SUS (2008) Review and comparison of nanofluid thermal conductivity and heat transfer enhancements. Heat Transf Eng 29:432–460

Yu W, France DM, Timofeeva EV, Singh D, Routbort JL (2010) Thermophysical property-related comparison criteria for nanofluid heat transfer enhancement in turbulent flow. Appl Phys Lett 96:213109